Since January 2020 Elsevier has created a COVID-19 resource centre with free information in English and Mandarin on the novel coronavirus COVID-19. The COVID-19 resource centre is hosted on Elsevier Connect, the company's public news and information website.

Journal of Electroanalytical Chemistry 878 (2020) 114733

Contents lists available at ScienceDirect

Journal of Electroanalytical Chemistry

journal homepage: www.elsevier.com/locate/jelechem

Charge transfer reaction mechanisms of epoxyketone and boronated peptides at glassy carbon and boron doped diamond electrodes

Catarina Sofia Henriques de Jesus [a], Teodor Adrian Enache [b], Victor Constantin Diculescu [b,*]

[a] Laboratory of Electroanalysis and Corrosion, Instituto Pedro Nunes, Coimbra, Portugal
[b] National Institute of Material Physics, Atomistilor 405A, 077125 Magurele, Romania

ARTICLE INFO

Article history:
Received 13 August 2020
Received in revised form 28 September 2020
Accepted 29 September 2020
Available online 30 September 2020

Keywords:
Carfilzomib
Delanzomib
Oprozomib
Redox mechanism
Glassy carbon
Boron doped diamond

ABSTRACT

The ubiquitin-proteasome system regulates the level of proteins within cells through controlled proteolysis. In some diseases, the system function is dysregulated turning the ubiquitin-proteasome complex into a target for drug development. The redox behavior of proteasome inhibitors, epoxyketone and boronated peptides carfilzomib, oprozomib and delanzomib was investigated by voltammetric methods using glassy carbon and boron doped diamond electrodes. It was showed that the oxidation of epoxyketone peptides carfilzomib and oprozomib occurred in one step at glassy carbon electrode surface while at boron doped diamond two consecutive charge transfer reactions due to different adsorption orientation at the electrode surface were observed. The moieties of these peptides, involved in the oxidation process, were morpholine for carfilzomib and thiazole for oprozomib. For the boronated peptide delanzomib, two irreversible and independent redox processes, oxidation at +0.80 V and reduction at −1.40 V were identified in neutral media at both electrodes. The oxidation reaction occurred at the amino group close to the pyridine moiety of delanzomib with the transfer of one electron and one proton whereas the reduction process takes place at pyridine ring in a two-electrons two-protons mechanism. Redox mechanisms were proposed and the implications on the proteasome inhibition discussed.

1. Introduction

In eukaryotic cells, the ubiquitin-proteasome system (UPS) controls the fundamental cellular processes by regulating the level of proteins within cells through controlled degradation, an important aspect of cell regulation [1]. The UPS components of mammals are ubiquitin, a small regulatory protein found in most tissues of eukaryotic organisms, and the cytosolic 26S proteasome which contains the 20S protein subunit and two 19S regulatory cap subunits [2]. Proteins targeted for degradation are recognized through their ubiquitin tag by the 19S cap structure of 26S proteasome and cleaved through proteolysis by the 20S subunit [1,2]. In some diseases including cancer, the UPS is dysregulated and the increased activity of proteasome results in excessive degradation of specific substrates, including the tumor suppressor p53 and the inhibitor of several nuclear factors, and affect several processes that drive tumor progression [3]. One of the standard strategy of disease control is represented by targeted therapy, in which the target drug is used for inhibition of proteasome activity [4]. Considering the specificities and affinities for the different catalytic sites within the proteasome core as well as their chemical structure and active moiety, the proteasome inhibitors may be divided into three groups: boronates, epoxyketones, and salinosporamides [4].

In 2003, bortezomib was approved as the first drug to be used on large scale as proteasome inhibitor. Although bortezomib showed severe secondary effects regarding the neurotoxicity it demonstrated an elevated clinical effectiveness, being the only new drug administered as mono-therapy that prolonged survival [5,6]. Due to the high interested on this types of therapeutic drugs, new inhibitors such carfilzomib in 2012 among others [7–10] were proposed. Also, a number of second-generation of inhibitors such as oprozomib and delanzomib, have been developed and are undergoing intense examination in clinical trials [9,11,12]. Nonetheless, it is important to mention that such compounds are used as inhibitors of other proteases, while recently, boron-containing compounds including delanzomib are tested as inhibitors of SARS-CoV-2 main protease [13].

As new developed drugs, the understanding of their physico-chemical properties represents an important step for elucidation of theirs's mechanism of action at biological level. The main characteristic feature of fundamental biological processes is represented by electron-transfer reactions and although the complexity of reactions varies considerably from case to case, the underlying principles that dictate the rate of electron transfer are the same. Consequently, the electrochemical methods can simulate the redox mechanisms providing insight about the electron-transfer reaction for new discovered molecules and lead to the development of

* Corresponding author.
E-mail address: victor.diculescu@infim.ro. (V.C. Diculescu).

http://dx.doi.org/10.1016/j.jelechem.2020.114733

analytical strategies for detection, quantitation, and elucidation of their redox mechanisms, the electrochemical investigation of new discovered proteasome inhibitors, carfilozomib, oprozomib and delanzomib can support the pharmacokinetic studies for understanding of their mechanism of action.

In this context, the aim of the present study is the investigation of the electron transfer properties of some newly discovered proteasome inhibitors, using voltammetric methods at glassy carbon and boron doped diamond electrodes. The investigation of the electrochemical redox mechanisms of carfilozomib, oprozomib and delanzomib, Scheme 1, has the potential for providing valuable insights into biological redox reactions of this class of molecules, resulting in a better understanding of physicochemical properties and their mechanisms of action at different rates and by different pathways.

2. Experimental

2.1. Materials and reagents

Carfilozomib, oprozomib, delanzomib, morpholine, methylmorpholine, 2-aminothiazole and 2-methylthiazole were purchased from Selleckchem, Munich, Germany. The electrolyte solutions of 0.1 M ionic strength were prepared with analytical grade reagents and purified water from a Millipore Milli-Q system (conductivity $\leq 0.1\ \mu S\ cm^{-1}$). The pH measurements were carried out with a Crison micropH 2001 pH-meter using an Ingold combined glass electrode. Microvolumes were measured using EP-10 and EP-100 Plus Motorized Microliter Pippettes (Rainin Instrument Co. Inc., Woburn, USA). All experiments were done at room temperature (25 ± 1 °C).

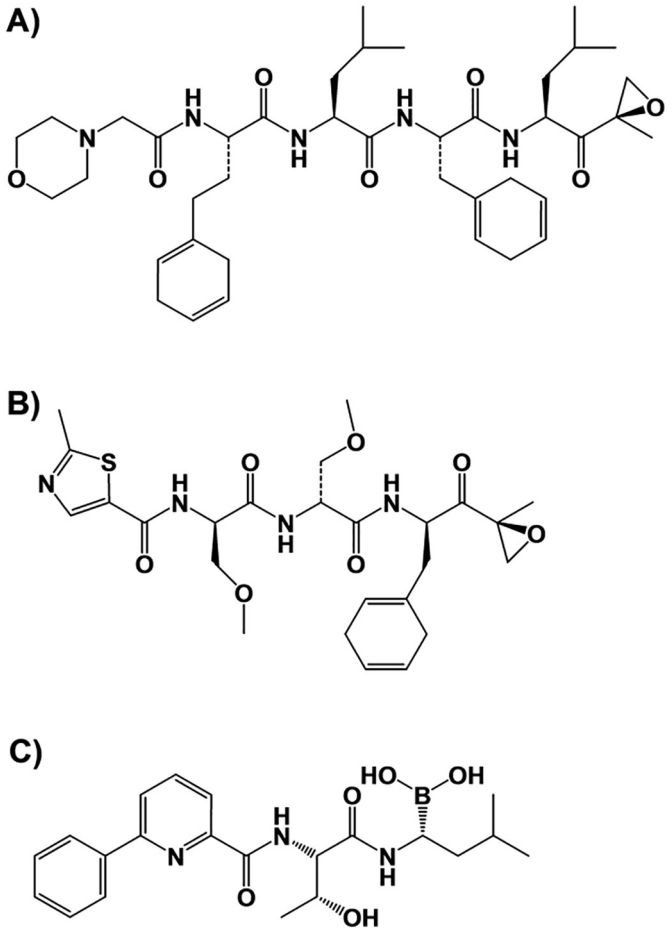

Scheme 1. Chemical structures of A) carfilzomib, B) oprozomib and C) delanzomib.

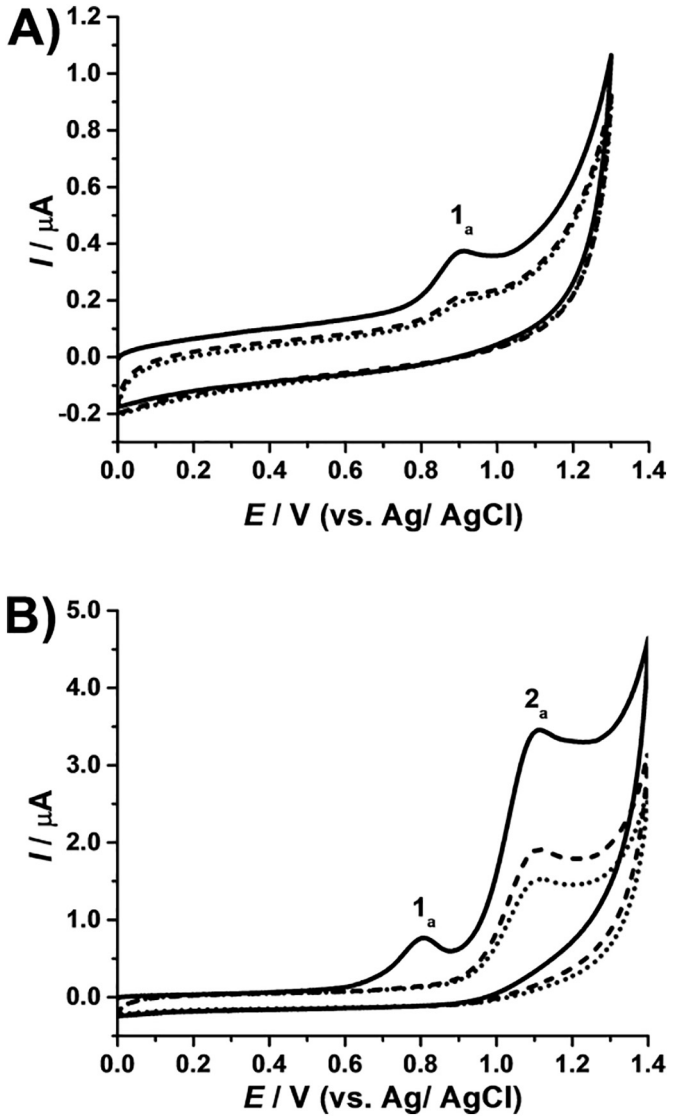

Fig. 1. Cyclic voltammogram with A) GCE and B) BDDE in solution of 25 μM carfilzomib in 0.1 M phosphate buffer pH = 7.0 at ν = 100 mV s^{-1}; () 1st, (…) 2nd and (…) 3rd scans.

2.2. Voltammetric parameters and electrochemical cells

Voltammetric experiments were carried out using an IVIUM potentiostat in combination with IviumSoft program version 2.219 (Ivium Technologies, Eindhoven, The Netherlands). Measurements were carried out using a working glassy carbon (GC) (0.79 mm^2) or a boron doped diamond (BDD) (25 mm^2), a counter Pt wire and an Ag/AgCl (3 M KCl) reference electrodes, in a one-compartment 2 mL electrochemical cell. The experimental conditions for differential pulse voltammetry (DPV) were: pulse amplitude 50 mV and pulse width 100 ms at a scan rate of 5 mV s^{-1}. For square wave voltammetry (SWV) a pulse of 50 mV, frequency of 25 and 50 Hz and a potential increment of 2 mV, corresponding to an effective scan rate of 50 and 100 mVs^{-1} were used.

The GCE was polished using diamond spray (particle size 1 μm) on a microcloth pad before each experiment. After polishing, the electrode was rinsed thoroughly with Milli-Q water for 30s; then it was placed and pretreated in the supporting electrolyte where various DP voltammograms were recorded until a steady state baseline voltammogram was obtained.

Prior to use, the BDD electrode was washed with ethanol and Milli-Q water, and the surface was activated in the supporting electrolyte using cyclic voltammetry between the potential limits of 0.0 V and + 2.5 V, until a

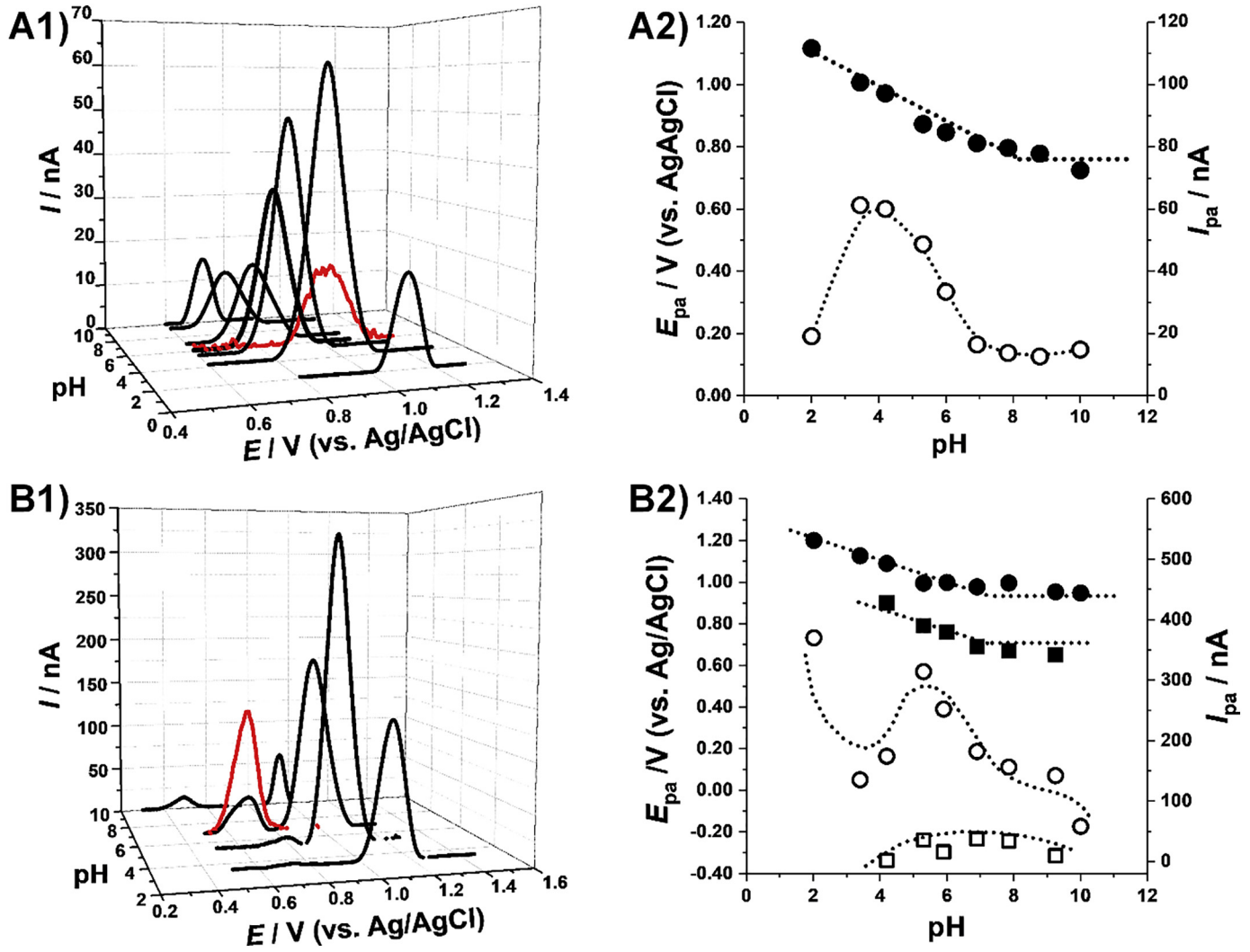

Fig. 2. 1) DP voltammogram in solution of 25 μM carfilzomib function of pH of the supporting electrolyte with A) GCE and B) BDDE. 2) Plots of the variation of (○,□) I_{pa} and (●,■) E_{pa} of carfilzomib vs. pH. The red curves correspond to voltammograms recorded in solutions of methyl-morpholine.

stable signal was detected (15–20 cycles at a potential scan rate of 150 mV s^{-1}). This procedure ensured very reproducible experimental results.

2.3. Acquisition and presentation of voltammetric data

All the DP and SW voltammograms presented were background-subtracted and baseline-corrected using the IviumSoft program tools. This mathematical treatment improves the visualization and identification of peaks over the baseline without introducing any artefact, although the peak height is in some cases reduced (<10%) relative to that of the untreated curve. Nevertheless, this mathematical treatment of the original voltammograms was used in the presentation of all experimental voltammograms for a better and clearer identification of the peaks. The values for peak current presented in all graphs were determined from the original untreated voltammograms after subtraction of the baseline.

3. Results

The electrochemical behavior of carfilzomib, oprozomib and delanzomib at glassy carbon and boron doped diamond electrodes was studied over a wide pH range by means of electrochemical techniques such as cyclic, differential pulse and square wave voltammetry.

3.1. Carfilzomib

3.1.1. Cyclic voltammetry

Cyclic voltammograms of 25 μM carfilzomib recorded at the GCE in 0.1 M phosphate buffer pH 7.0 between potential limits 0.0 V and + 1.40 V, at ν = 100 mV s^{-1} revealed a single oxidation reaction, corresponding to peak 1_a at +0.90 V, Fig. 1A. By recording successive voltammograms in the same solution and without cleaning the GCE surface it was observed a decrease of the oxidation current of peak 1_a, explained by the adsorption of carfilzomib oxidation products at the GCE surface reducing the electroactive area. No additional signals were observed meaning that the oxidation products of carfilzomib are not electroactive. Increasing the negative potential limit, until −1.20 V no cathodic peaks appeared (data not shown).

Scan rate studies were carried out in order to understand if the oxidation process is controlled by diffusion or by adsorption. The effect of scan rate on the oxidation of 10 μM carfilzomib was evaluated in phosphate buffer pH = 7.0 (data not shown). Increasing the scan rate, the peak potential shifted to more positive values. The variation of the peak current with scan rate in the range of 25–500 mV s^{-1} followed the first degree equation I_{pa} / nA = −8.6 + 389.2 × ν / V s^{-1} (R^2 = 0.991), while with square root of the scan rate the second degree equation I_{pa} / nA = −0.1 + 34.1 × (ν / V s^{-1}) + 426.3 × (ν / V s^{-1})^2 (R^2 = 0.997). Also, the logarithm of the peak current varied linearly with the logarithm of the scan rate in

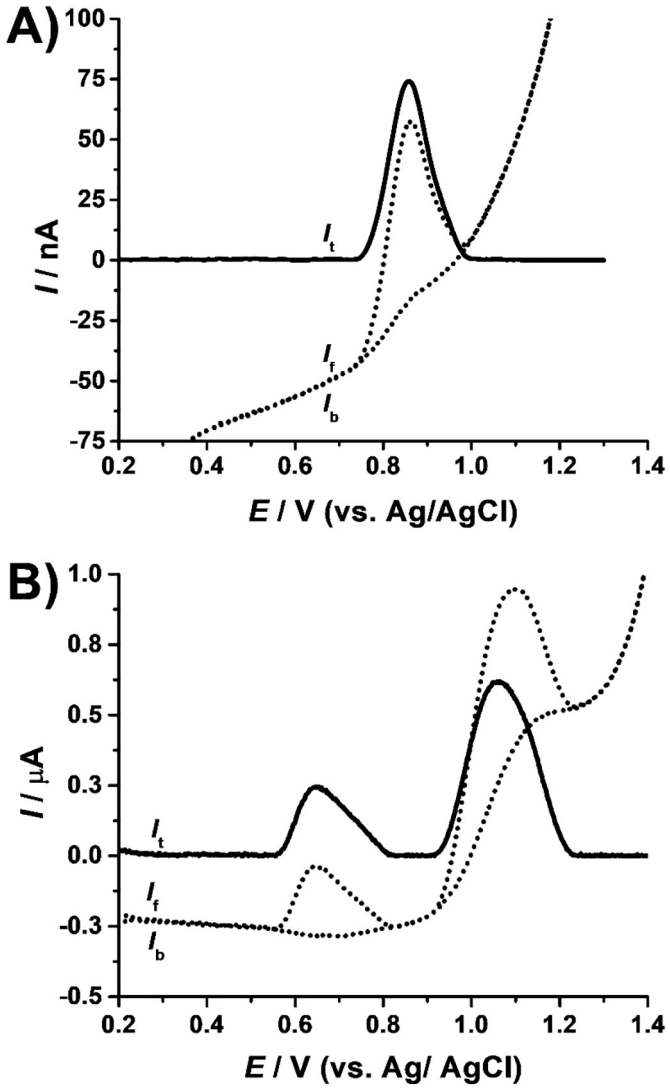

Fig. 3. SW voltammograms with A) GCE and B) BDDE in solution of 25 μM carfilzomib in 0.1 M phosphate buffer pH = 7.0 at ν = 100 mV s^{-1}.

agreement with $\log(I_{pa}/\text{nA}) = -6.4 + 1.1 \times \log(\nu/\text{V s}^{-1})$ ($R^2 = 0.991$), showing that the oxidation of carfilzomib involves adsorption of the compound at the GCE surface.

Cyclic voltammograms were also recorded at the BDD working electrode, Fig. 1B. The oxidation of 25 μM carfilzomib recorded at ν = 100 mVs^{-1} revealed two anodic charge reactions, peak 1_a at +0.80 V and peak 2_a at + 1.10 V. Recording successive voltammograms in the same solution, without cleaning the electrode surface, the oxidation peak 1_a disappears while the second oxidation peak occurred with a lower current intensity. Although it is known that the adsorption of chemical species at BDD surface is low, the disappearance of peak 1_a, as well as the decrease of the second peak can be explained by the adsorption of oxidation products at the sp^2 regions of BDD, reducing the available electroactive surface.

The cyclic voltamograms obtained for 25 μM carfilzomib in supporting electrolytes with different pH values showed that carfilzomib oxidation is a pH-dependent reaction (data not shown).

3.1.2. Differential pulse voltammetry

Due to the high sensitivity of DPV when compared with cyclic voltammetry, the pH effect on the electrochemical oxidation of carfilzomib was investigated for electrolytes with 2.0 < pH < 10.0, using DP voltammetry.

DP voltammograms were recorded with the GC and BDD electrodes in solutions of 25 μM carfilzomib in electrolytes with different pH values, Fig. 2 A1. Similar to cyclic voltammetry experiments, at GC electrode only peak 1_a was observed. For pH < 7.0, the peak potential was pH dependent and shifted linearly to less positive values with increasing pH, following the relationship E_{pa} = 1.22–0.06 pH, Fig. 2 A2. The slope of −60 mV per pH unit was in agreement with an oxidation reaction that involves the transfer of the same number of electrons and protons. Taking into account the width at the half height of the peak of approx. 100 mV it can be concluded that the oxidation reaction of carfilzomib at GC electrode, for pH lower than 7, occurred with the transfer of one electron and one proton. Increasing the pH of the solution above 7, the peak potential turned pH independent, in agreement with a mechanism that involves only the transfer of electrons.

On the DP voltammograms recorded with the BDDE in solutions of 25 μM carfilzomib in electrolytes with different pH values two charge transfer reactions corresponding to peaks 1_a and 2_a were observed, Fig. 2 B1. For pH < 7.0 the peak potentials were pH dependent and shifted linearly to less positive values with increasing pH, Fig. 2 B2.

The relationship for peak 1_a was E_{p1a} = 1.34–0.06 pH and for peak 2_a E_{p1a} = 1.12–0.06 pH. The slopes of −60 mV per pH unit was in agreement with the transfer of the same number of electrons and protons. For pH > 7.0 the peak did not vary with the pH of the supporting electrolyte meaning that the oxidation involved only the transfer of electrons and no proton.

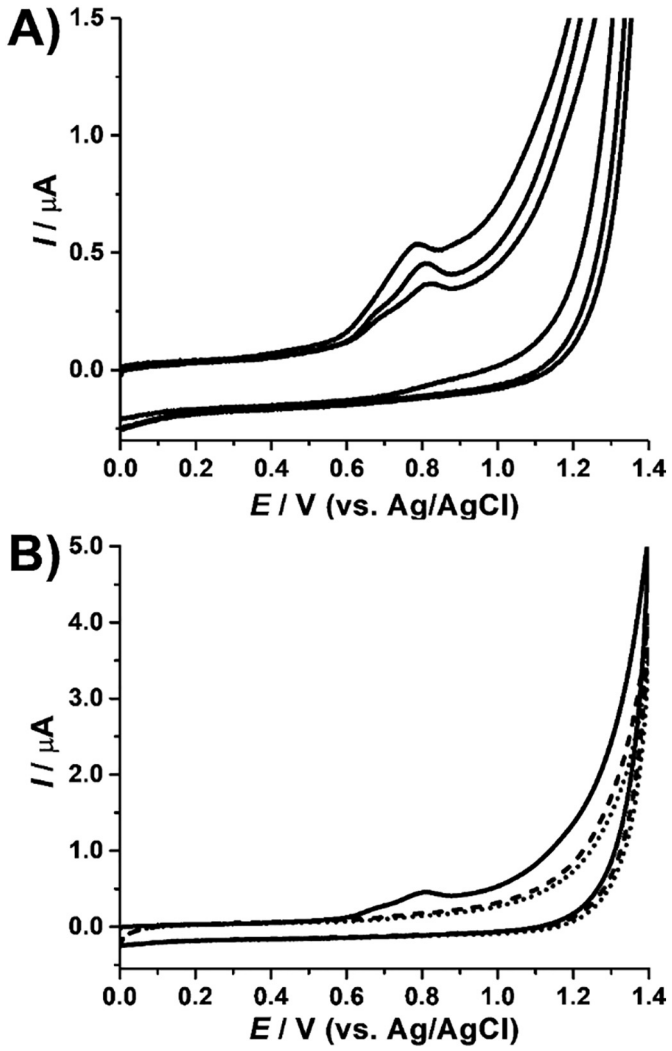

Fig. 4. Cyclic voltammogram with BDDE in solution of: A) different concentrations and B) 100 μM oprozomib (—) 1st, (…) 2nd and (…) 3rd scans, in 0.1 M phosphate buffer pH = 7.0 at ν = 100 mV s^{-1}.

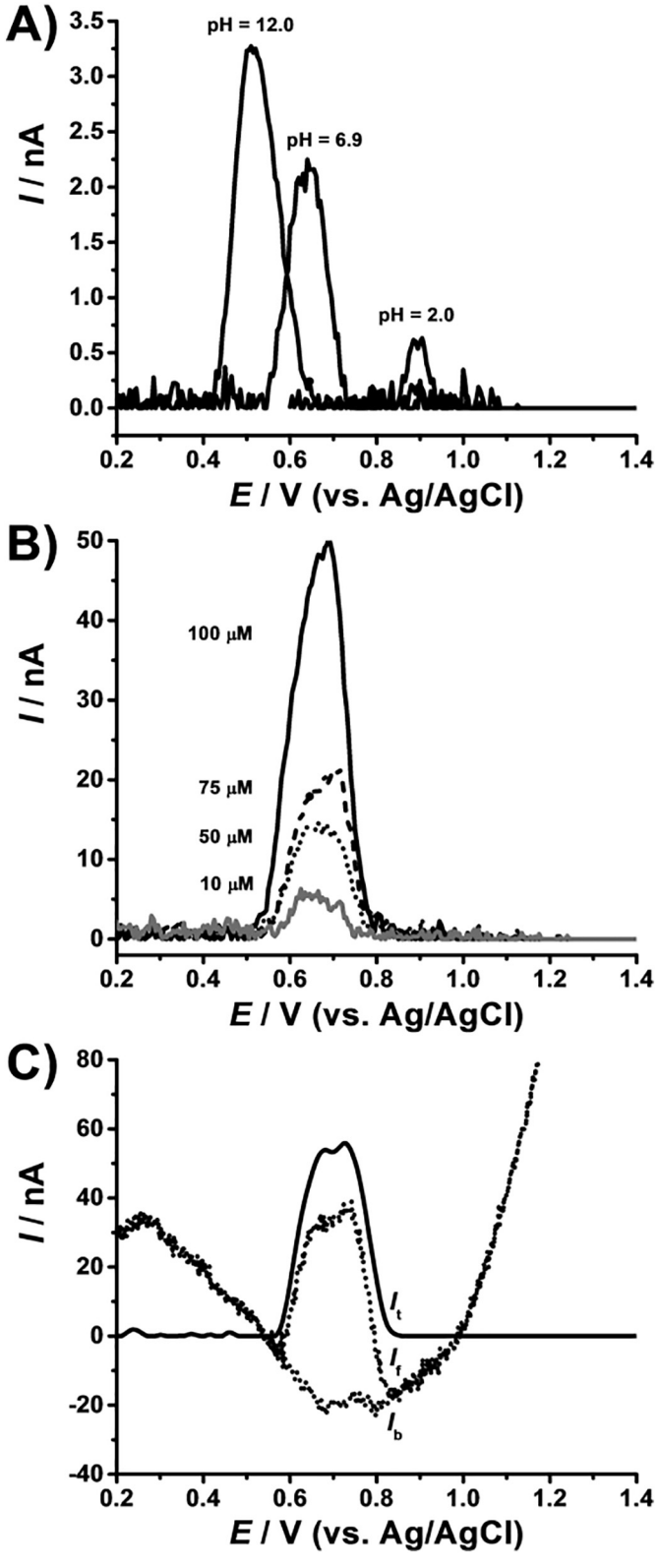

Fig. 5. A, B) DP and C) SW voltammograms with A) GCE and B,C) BDDE in solutions of A) 75 μM oprozomib in electrolytes with different pH values, B) different concentrations of oprozomib in 0.1 M phosphate buffer pH = 7.0, and C) 75 μM oprozomib in 0.1 M phosphate buffer pH = 7.0. For SWV, I_t, I_b and I_f represents the total, backward and forward currents.

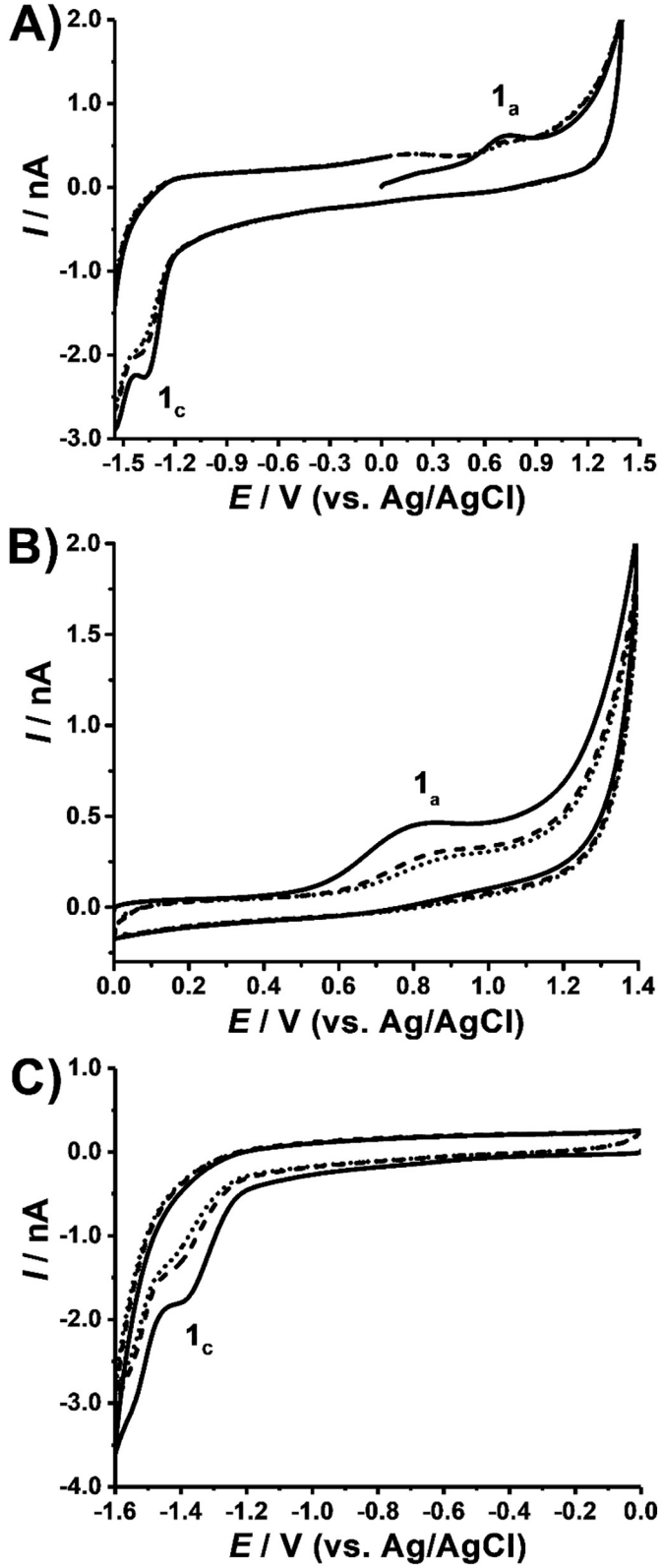

Fig. 6. Cyclic voltammograms obtained with GCE in solutions of 200 μM delanzomib in 0.1 M phosphate buffer pH = 7.0 between potential limits of: A) + 1.40 and − 1.50 V; B) 0 and + 1.40 V; and C) 0 and − 1.60 V; ν = 100 mV s^{-1}; (—) 1st, (…) 2nd and (…) 3rd scans.

3.1.3. Square wave voltammetry

In SWV the current is sampled in both positive and negative-going pulses, oxidation and reduction peaks of the electroactive compound can be obtained simultaneously, and the reversibility of the electron transfer reaction monitored by plotting the forward and backward components of the total current. In order to verify if the redox process of carfilzomib is either

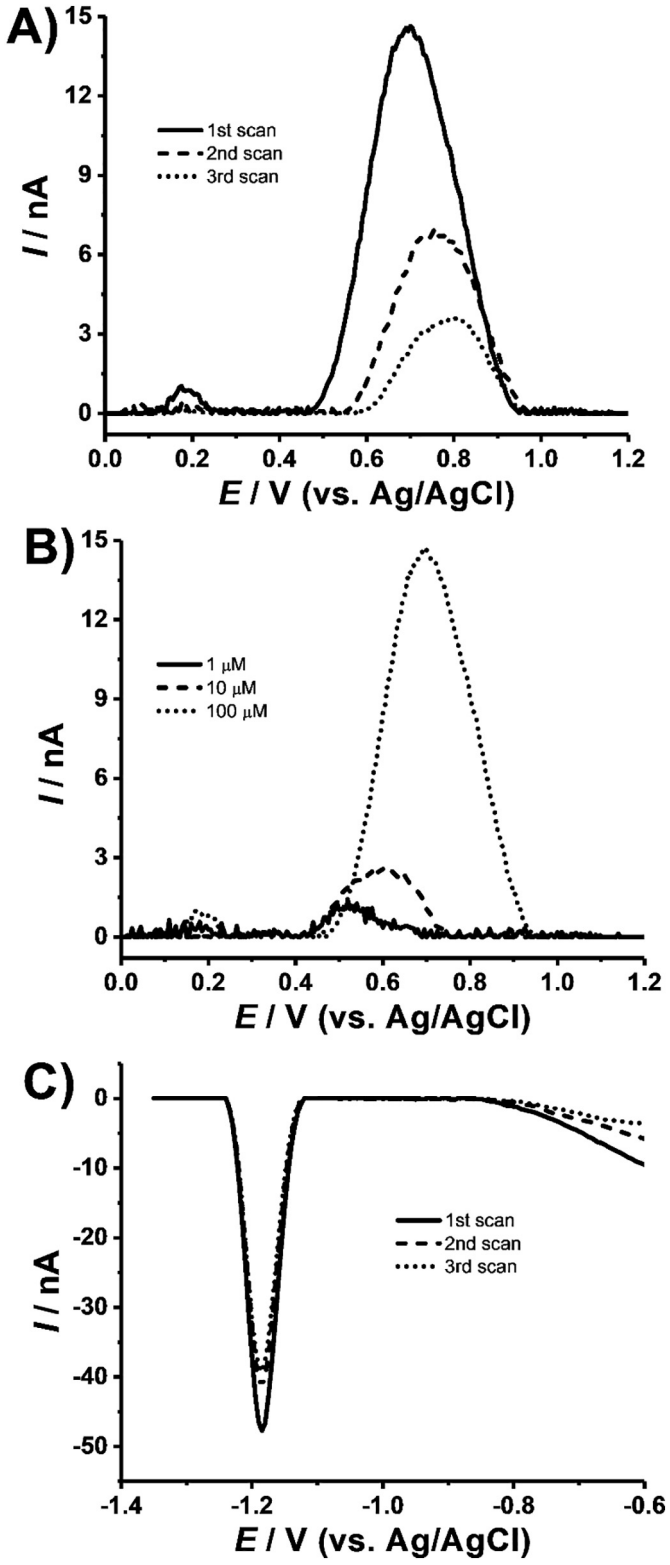

Fig. 7. DP voltammograms obtained with GCE in solution containing different concentration of delanzomib in 0.1 M phosphate buffer pH = 7.0: A) (—) 1st, (…) 2nd and (…) 3rd anodic scan for 200 μM; B) first scan for (—) 1, (…) 10 and (…) 100 μM and **C)** (—) 1st, () 2nd and (…) 3rd cathodic scan in 200 μM delanzomib.

reversible or irreversible, SW voltammograms were recorded in 25 μM carfilzomib with both GCE and the BDD.

The deconvolution of the total current recorded at the GCE into the forward and backward components showed peaks corresponding to oxidation processes, Fig. 3A. The forward and backward components of the total current recorded with the BDD showed manly oxidation peaks with low cathodic correspondents, Fig. 3B.

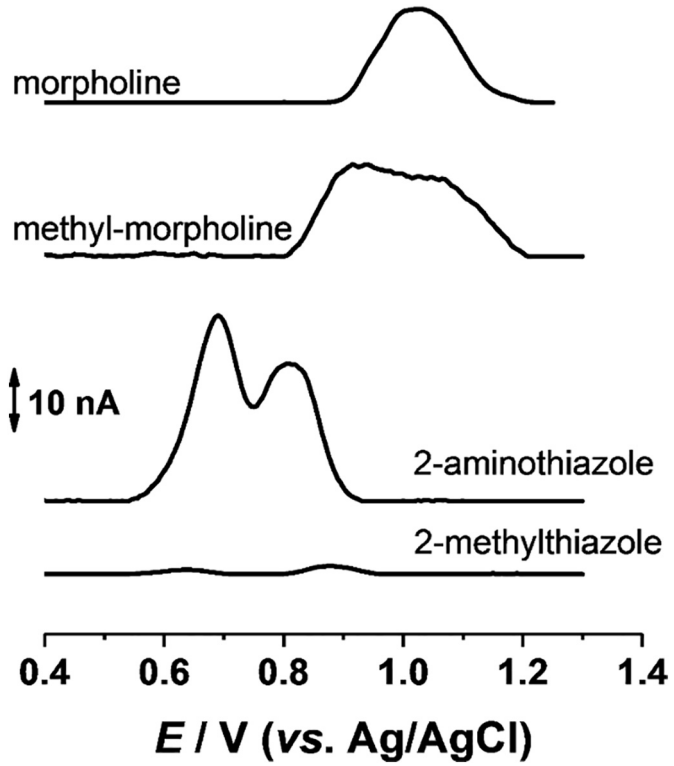

Fig. 8. DP voltammograms recorded at GCE in 100 μM morpholine and methylmorpholine, and in 10 μM 2-aminothiazole and 2-methylthiazole in 0.1 M phosphate buffer pH = 7.0.

3.2. Oprozomib

3.2.1. Cyclic voltammetry

The CV results obtained for oprozomib at GC electrode showed no anodic or cathodic peak even for elevated concentration. However, the use of BDD electrode allowed the investigation of the electrochemical behavior of oprozomib.

Cyclic voltammograms were recorded in 0.1 M phosphate buffer pH 7.0 at BDDE for different concentration of oprozomib. At low concentration, two oxidation peaks were identified, at +0.67 V and + 0.82 V, and by increasing the concentration the peaks tend to merge into one. Reversing the scan direction, no cathodic charge transfer was observed, Fig. 4A. Recording successive voltammograms in the same solution without cleaning the electrodes surface, the oxidation peaks of oprozomib disappear and no additional peaks were observed, meaning that the oxidation product is not electroactive Fig. 4B.

3.2.2. Differential pulse voltammetry

DP voltammograms were recorded with the GCE in solutions of 75 μM oprozomib in electrolytes with different pH values. In all voltammograms, it was observed only one main oxidation peak. The both components of the peak, oxidation potential and current, were pH-dependent: the oxidation potential shifts to lower values and the oxidation current increased with the increase of the pH value of the supporting electrolyte, Fig. 5A. However, the highest oxidation current values obtained at pH = 12.0 was around 3.5 nA.

In order to achieve a higher sensitivity BDD electrode was used and DP voltammograms were recorded in pH 7.0 for different concentrations of oprozomib. For all concentration investigated, two consecutive charge transfer reactions occurred at +0.62 V and + 0.71 V, Fig. 5B, and

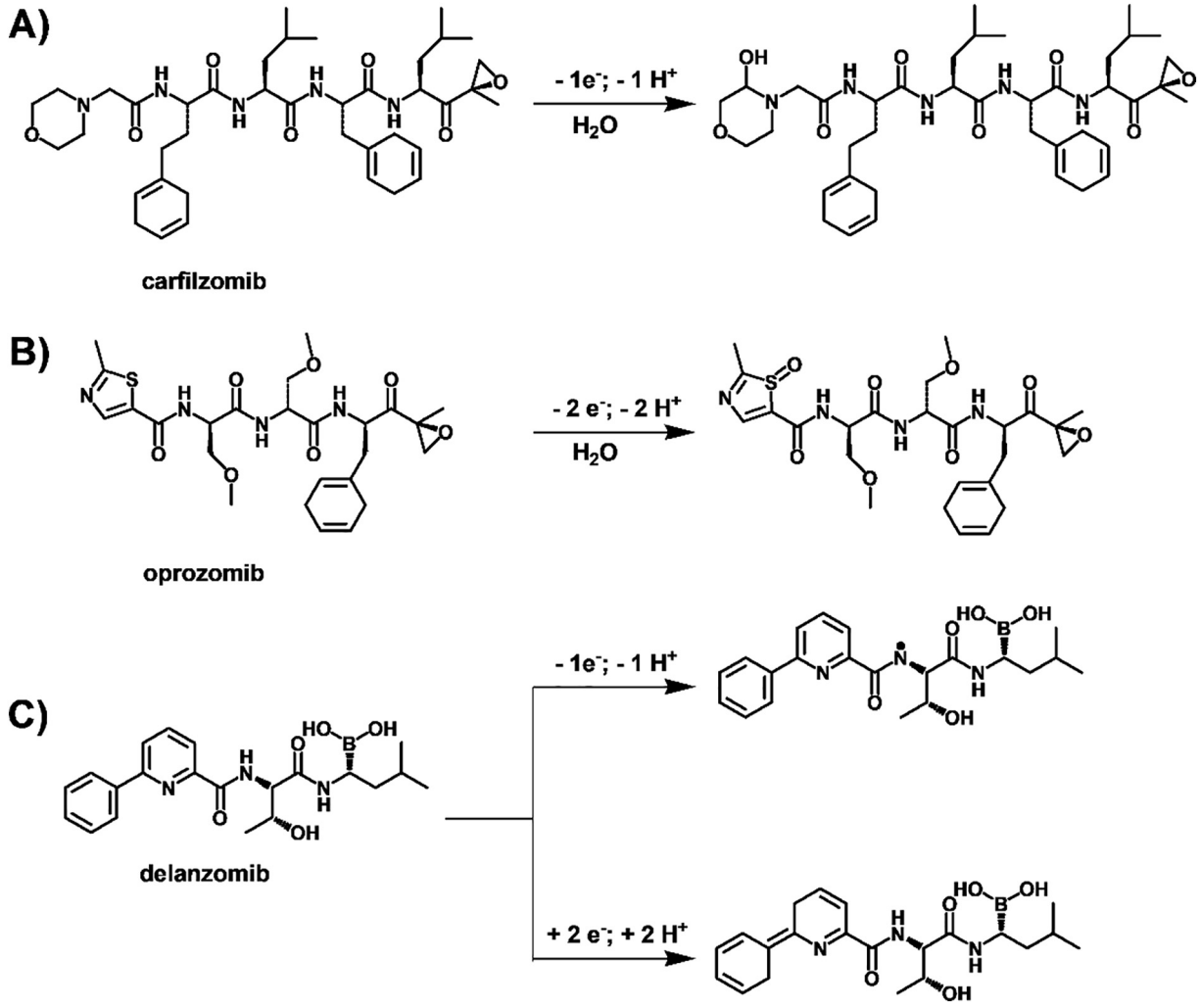

Scheme 2. Proposed redox mechanisms for A) carfilzomib, B) oprozomib and C) delanzomib.

recording consecutive voltammograms in the same solution without cleaning the leaded to the decrease of both oxidation peaks.

3.2.3. Square wave voltammetry

In order to investigate the reversibility of the oxidation reaction of oprozomib, SW voltammograms were recorded at pH 7.0 in 75 μM oprozomib at BDD electrode. On the SW voltammograms both consecutive charge transfers reactions occurred, Fig. 5C. The deconvolution of the total current showed high peaks corresponding to oxidation and small signals to reduction processes in agreement with the quasi-reversibility of the reaction.

3.3. Delanzomib

3.3.1. Cyclic voltammetry

The voltammetric behavior of 200 μM delanzomib at the GCE was investigated by cyclic voltammetry in phosphate buffer pH 7.0, in a N_2-saturated solution, Fig. 6. During the voltammetric measurements a constant flux of N_2 was kept over the solution in order to avoid the diffusion at atmospheric O_2 into the delanzomib solution.

On the positive-going scan recorded from 0.00 V till +1.40 V one main anodic peak 1_a occurred at +0.70 V, Fig. 6 A and B. On the negative-going scan, a reduction peak 1_c appeared at −1.35 V, Fig. 6A. Recording successive voltammograms in the same solution and without cleaning the electrode surface, the anodic and cathodic peaks of delanzomib decreased with the increase number of scan due to the adsorption of redox products, which decreased the electroactrive area of GC electrode surface. In addition, the negative-going scan recorded at a clean GC electrode surface between 0.0 V and − 1.40 V showed the peak 1_c at −1.35 V. Therefore, it can be concluded that the oxidation and the reduction of delanzomib occurred independently of each other, Fig. 6C.

3.3.2. Differential pulse voltammetry

The redox behavior of delanzomib at GC electrode was also investigated by means of DPV. The DP anodic voltammogram recorded at GC in pH 7.0 for a solution containing 100 μM delanzomib showed one oxidation peak occurring at +0.70 V with a current intensity of 15 nA, Fig. 7A. Increase the number of voltammograms recorded in the same solution and without cleaning the electrode surface a decrease of the oxidation peak current occurred simultaneous with a positive oxidation potential shift with the increase number of scans, Fig. 7A, confirming the fact that oxidation products adsorb on the electrode surface, decreasing the electroactive available area and making more difficult the oxidation of delanzomib molecules.

Moreover, it was observed that increasing the delanzomib concentration results in a positive potential shift, Fig. 7B, a phenomenon associated with the adsorption and the orientation of molecules at the electrode surface.

The cathodic DP voltammograms presented the reduction peak 1_c of delanzomib occurring at −1.18 V. Subsequent scans recorded without cleaning the electrode surface showed only a small decrease of the reduction current while the potential remains the same, in agreement with a diffusion-drive process with no or very small adsorption of reaction products at the electrode surface.

4. Discussion

The experiments above described demonstrated that the epoxyketone peptides carfilzomib and oprozomib as well as the boronated peptide delazomib undergo electrochemical redox reactions.

Referring to the epoxyketones, carfilzomib undergoes one electron and one proton electrochemical oxidation while the oxidation of oprozomib involves the transfer of two electrons and two protons. This indicates the existence of different electroactive centres and redox mechanisms. In order to obtain detailed information on their redox mechanism, experiments were carried out in solutions of morpholine and methyl-morpholine for carfilzomib, and in 2-aminothiazole and 2-methylthiazole for oprozomib.

The DP voltammograms recorded in solutions of morpholine and methyl-morpholine, Fig. 8**,** showed that both compounds undergo oxidation at potential values close to those of carfilzomib, Fig. 2A and C (red lines). These experiments proved that the oxidation of carfilzomib occurred with the transfer of one electron and one proton from the morpholine moiety, Scheme 2A. Although the epoxy moiety was demonstrated to undergo redox reactions [14], this group was not involved into the redox mechanisms of carfilzomib. However, the epoxy moiety can influence the adsorption and orientation of molecules and/or their redox products at the electrode surface. Nevertheless, the occurrence of two oxidation peaks on the voltammograms recorded with the BDDE is explained considering the embedded sp^2 graphite domains into the diamond structure [15] which lead to the adsorption of carfilzomib at BDD surface in different orientations that facilitate the electron transfer reactions when compared to the GCE.

Likewise, the DP voltammogram recorded in buffer after adsorption in solutions of 2-aminothiazole and 2-methylthiazole, Fig. 8, showed two consecutive charge transfer reactions at potential values close to those obtained for oprozomib. Considering the results presented above, it is proposed that the oxidation of oprozomib involves the thiazole moiety. Thus, the overall transfer of two electrons and two protons from the sulphur atom in the presence of water leads to the formation of sulfoxide. On its turn, the sulfoxide group undergoes electrochemical oxidation in the presence of water resulting in a sulfone [16], Scheme 2B.

Referring to the boronated peptide delanzomib, its electrochemical oxidation occurs in a one-step irreversible mechanism. The electrochemistry of boron-containing compounds is well documented [17] but in the case of delanzomib, at least in the present experimental conditions, the boronic acid moiety does not represent an electroactive centre. Instead, the redox behavior of delanzomib was compared to that of bortezomib [18]. The similarities observed indicated that the oxidation of delanzomib corresponds to that of the aliphatic secondary amide. Thus, the anodic reaction, Scheme 2C, involves the transfer of one electron and one proton leading to the formation of a radical, which undergoes homogenous chemical reactions. On the other hand, the reduction of delanzomib occurs in a one-step irreversible mechanism, Scheme 2C, involving the transfer of two electrons and two protons and the reaction is taking place at the phenylpyridine ring.

Generally, the inihibition mechanism of the proteasome by the epoxyketones and the boronated peptides involves a threonine residue in the catalytic site. For example, in the case of oprozomib and carfilzomib, a morpholino ring is formed via a dual covalent interaction between Nα and Oγ of the threonine residue, and the C-terminal epoxyketone group. In the case of delanzomib and bortezomib, the formation of a tetrahedral hydrogen-bond between boronic acid moiety and threonine residue is described. From the experiments described in this research, it is evident that none of the moieties can be affected by oxidation. However, it can be inferred that the oxidation product of delanzomib, as an unstable radical can readily interact with any other amino acid residue in the enzyme structure or, more generally, any other cellular component [19,20]. On their turn, the N-terminal morpholine moiety of carfilzomib or the thiazole moiety in case of oprozomib, which represents the electroactive sites of these compounds, are not involve in any interaction with the catalytic site. However, these groups are involved in the stabilization of the peptide's backbone in the molecular complex formed after the interaction of epoxyketone with the threonine residue of the catalytic site [21]. Also, in this case it can be inferred that the hydroxyl group formed after oxidation of carfilzomib as well as the formation of the sulfoxide in the case of oprozomib can interfere with other electrophilic anchors altering the compound 3D conformation, the interaction with the amino acid residues in the catalytic site, and consequently their inhibiting properties.

5. Conclusions

The voltammetric behavior of proteasome inhibitors epoxyketones carfilzomib and oprozomib, and the boronated peptide delanzomib was investigated by cyclic, differential pulse and square wave voltammetry at glassy carbon and boron doped diamond electrodes in different electrolyte media and at different concentrations of analytes.

The oxidation of the epoxyketone peptide carfilzomib took place in one step but at the boron doped diamond electrode two peak currents were observed due to different orientations of the molecule at the electrode surface. The voltammetric results indicated that the electrochemical oxidation of carfilzomib occurred at the morpholine ring with the transfer of one electron and one proton in an adsorption controlled pH-dependent mechanism. This mechanism was confirmed by investigation of the redox properties of morpholine and methyl-morpholine.

The epoxyketone peptide oprozomib showed a very weak electroactivity at glassy carbon electrode but the use of boron doped diamond electrode revealed that the oxidation occurred with the transfer of two electrons and two protons. Comparative investigations with -aminothiazole and 2-methylthiazole, demonstrated that the thiazole moiety of oprozomib is involved in the anodic charge transfer reaction leading to the formation of a sulfone.

The electrochemical oxidation of the boronated peptide delanzomib showed similar behavior at both glassy carbon and boron doped diamond electrodes. It was demonstrated that, at pH 7.0, delanzomib can be oxidized and reduced in independent reactions. The electroactive center corresponding to the oxidation was identified to be an amino group while for the reduction reaction the phenylpyridine moiety.

Author contributions

Catarina Sofia Henriques de Jesus: Data curation, Formal analysis, Investigation, Methodology, Writing - original draft. Teodor Adrian Enache: Data curation, Formal analysis, Investigation, Methodology, Writing - original draft, Writing-Reviewing and Editing. Victor C. Diculescu: Conceptualization, Formal analysis, Funding acquisition, Investigation, Methodology, Project administration, Resources, Supervision, Writing - original draft, Writing - review & editing.

Declaration of Competing Interest

The authors declare that they have no known competing financial interests or personal relationships that could have appeared to influence the work reported in this paper.

Acknowledgment

Financial support from the Romanian Ministry of Research and Innovation through Operational Programme Competitiveness 2014-2020 Project NANOBIOSURF-SMIS 103528, and from Fundação para a Ciência e Tecnologia (FCT) – Portugal through PTDC/DTP-FTO/0191/2012 is gratefully acknowledged.

References

[1] W. Heinemeyer, P.C. Ramos, R.J. Dohmen, Ubiquitin-proteasome system, Cell. Mol. Life Sci. 61 (2004) 1562–1578, https://doi.org/10.1007/s00018-004-4130-z.
[2] A. Ciechanover, Intracellular protein degradation: from a vague idea thru the lysosome and the ubiquitin–proteasome system and onto human diseases and drug

targetingNobel lecture 2004, © the Nobel foundation 2004, Cell Death Differ. 12 (2005) 1178–1190, https://doi.org/10.1038/sj.cdd.4401692.
[3] B. Cao, X. Mao, The ubiquitin-proteasomal system is critical for multiple myeloma: implications in drug discovery, Am. J. Blood Res. 1 (2011) 46–56.
[4] P. Moreau, P.G. Richardson, M. Cavo, R.Z. Orlowski, J.F. San Miguel, A. Palumbo, J.-L. Harousseau, Proteasome inhibitors in multiple myeloma: 10 years later, Blood 120 (2012) 947–959, https://doi.org/10.1182/blood-2012-04-403733.
[5] S. Grosicki, A. Barchnicka, A. Jurczyszyn, A. Grosicka, Bortezomib for the treatment of multiple myeloma, Expert. Rev. Hematol. 7 (2014) 173–185, https://doi.org/10.1586/17474086.2014.899144.
[6] H. Ma, Z. Su, F. Sun, N. Zhao, The activity and safety of novel proteasome inhibitors strategies (single, doublet and triplet) for relapsed/refractory multiple myeloma, Acta Oncol. (Madr). 57 (2018) 290–296, https://doi.org/10.1080/0284186X.2017.1364868.
[7] D. Ribatti, A historical perspective on milestones in multiple myeloma research, Eur. J. Haematol. 100 (2018) 221–228, https://doi.org/10.1111/ejh.13003.
[8] D.S. Siegel, T. Martin, M. Wang, R. Vij, A.J. Jakubowiak, S. Lonial, S. Trudel, V. Kukreti, N. Bahlis, M. Alsina, A. Chanan-Khan, F. Buadi, F.J. Reu, G. Somlo, J. Zonder, K. Song, A.K. Stewart, E. Stadtmauer, L. Kunkel, S. Wear, A.F. Wong, R.Z. Orlowski, S. Jagannath, A phase 2 study of single-agent carfilzomib (PX-171-003-A1) in patients with relapsed and refractory multiple myeloma, Blood 120 (2012) 2817–2825, https://doi.org/10.1182/blood-2012-05-425934.
[9] K. Zhang, A. Desai, D. Zeng, T. Gong, P. Lu, M. Wang, Magic year for multiple myeloma therapeutics: Key takeaways from the ASH 2015 annual meeting, Oncotarget 8 (2017) 10748–10759, https://doi.org/10.18632/oncotarget.13314.
[10] M.A. Dimopoulos, H. Goldschmidt, R. Niesvizky, D. Joshua, W.-J. Chng, A. Oriol, R.Z. Orlowski, H. Ludwig, T. Facon, R. Hajek, K. Weisel, V. Hungria, L. Minuk, S. Feng, A. Zahlten-Kumeli, A.S. Kimball, P. Moreau, Carfilzomib or bortezomib in relapsed or refractory multiple myeloma (ENDEAVOR): an interim overall survival analysis of an open-label, randomised, phase 3 trial, Lancet Oncol. 18 (2017) 1327–1337, https://doi.org/10.1016/S1470-2045(17)30578-8.
[11] A. Spencer, S. Harrison, J. Zonder, A. Badros, J. Laubach, K. Bergin, A. Khot, T. Zimmerman, D. Chauhan, N. Levin, A. MacLaren, S.D. Reich, M. Trikha, P. Richardson, A phase 1 clinical trial evaluating marizomib, pomalidomide and low-dose dexamethasone in relapsed and refractory multiple myeloma (NPI-0052-107): final study results, Br. J. Haematol. 180 (2018) 41–51, https://doi.org/10.1111/bjh.14987.
[12] B.A. Teicher, J.E. Tomaszewski, Proteasome inhibitors, Biochem. Pharmacol. 96 (2015) 1–9, https://doi.org/10.1016/J.BCP.2015.04.008.
[13] I.R. Vega Valdez, J.M. Santiago-Quintana, M. ROSALEZ, E. Farfan, M.A. Soriano-Ursua, Theoretical evaluation of bortezomib and other boron-containing compounds as inhibitors of SARS-CoV-2 main protease, 2020, https://doi.org/10.26434/CHEMRXIV.12047346.V1.
[14] A.G. Marrani, A. Motta, R. Schrebler, R. Zanoni, E.A. Dalchiele, Insights from experiment and theory into the electrochemical reduction mechanism of graphene oxide, Electrochim. Acta 304 (2019) 231–238, https://doi.org/10.1016/j.electacta.2019.02.108.
[15] T.A. Enache, A.-M. Chiorcea-Paquim, O. Fatibello-Filho, A.M. Oliveira-Brett, Hydroxyl radicals electrochemically generated in situ on a boron-doped diamond electrode, Electrochem. Commun. 11 (2009) 1342–1345, https://doi.org/10.1016/J.ELECOM.2009.04.017.
[16] T.A. Enache, A.M. Oliveira-Brett, Boron doped diamond and glassy carbon electrodes comparative study of the oxidation behaviour of cysteine and methionine, Bioelectrochemistry 81 (2011) 46–52, https://doi.org/10.1016/J.BIOELECHEM.2011.02.001.
[17] J.H. Morris, H.J. Gysling, D. Reed, Electrochemistry of boron compounds, Chem. Rev. 85 (1985) 51–76, https://doi.org/10.1021/cr00065a003.
[18] D.A. Golea, V.C. Diculescu, L. Tugulea, A.M. Oliveira Brett, Proteasome inhibitor anticancer drug Bortezomib redox behaviour at a glassy carbon electrode, Electroanalysis. 24 (2012) 1915–1921, https://doi.org/10.1002/elan.201200307.
[19] C. Richter, J.W. Park, B.N. Ames, Normal oxidative damage to mitochondrial and nuclear DNA is extensive, Proc. Natl. Acad. Sci. U. S. A. 85 (1988) 6465–6467, https://doi.org/10.1073/PNAS.85.17.6465.
[20] R.A. Floyd, J.M. Carney, Free radical damage to protein and DNA: mechanisms involved and relevant observations on brain undergoing oxidative stress, Ann. Neurol. 32 (1992) S22–S27, https://doi.org/10.1002/ana.410320706.
[21] W. Harshbarger, C. Miller, C. Diedrich, J. Sacchettini, Crystal structure of the human 20S proteasome in complex with Carfilzomib, Structure 23 (2015) 418–424, https://doi.org/10.1016/J.STR.2014.11.017.